

Light Front Cloudy Bag Model: Nucleon Electromagnetic Form Factors

Gerald A. Miller

Department of Physics, University of Washington
Seattle, WA 98195-1560

E-mail: miller@phys.washington.edu

October 24, 2018

Abstract

The nucleon is modeled, using light front dynamics, as a relativistic system of three bound constituent quarks emersed in a cloud of pions. The pionic cloud is important for understanding low-momentum transfer physics, especially the neutron charge radius, but the quarks are dominant at high values of Q^2 . The model achieves a very good description of existing data for the four electromagnetic elastic form factors.

The recent exciting experimental results for the ratio proton elastic form factors G_E/G_M (or QF_2/F_1)[1, 2] and the impending high accuracy data for the neutron electric[3] and magnetic[4] form factors have re-ignited interest in the venerable goal of understanding the structure of the nucleon.

The aim of the present paper is to present a reasonable, workable model which describes currently available information and makes predictions testable against data taken at higher values of Q^2 , or taken for improved accuracy. The model should have enough content so that its ultimate disagreement with experiment elucidates some missing piece of physics. Poincaré invariance and chiral symmetry are the principal tools used to construct the model.

Poincaré invariance is maintained or approximated by using light-front dynamics, in which fields are quantized at a fixed “time”= $\tau = x^0 + x^3 \equiv x^+$. The τ -development operator is then given by $P^0 - P^3 \equiv P^-$. The canonical spatial variable is $x^- = x^0 - x^3$, with a canonical momentum $P^+ = P^0 + P^3$. The other coordinates are \mathbf{x}_\perp and \mathbf{P}_\perp . The relation between energy and momentum of a free particle is given by: $p^- = \frac{p_\perp^2 + m^2}{p^+}$, a relativistic kinetic energy which does not contain a square root operator. This allows the separation of center of mass and relative coordinates, so that the computed wave functions are frame independent. The use of the light front is particularly relevant for calculating form factors, which are probability amplitudes for an nucleon to absorb a four momentum q and remain a nucleon. The initial and final nucleons have different total momenta. This means that the final nucleon is boosted relative to the initial one, and therefore has a different wave function. The light front technique allows one to use boosts that are independent of interactions.

We are concerned with the Dirac F_1 and Pauli F_2 ($F_2(0) = \kappa$, the anomalous magnetic moment) form factors. The Sachs form factors are $G_E = F_1 - Q^2/4M_N^2 F_2$, $G_M = F_1 + F_2$. We use the current’s “good” component, J^+ , so that $F_1(Q^2) = \langle N, \uparrow | J^+ | N, \uparrow \rangle$, $QF_2(Q^2) = (-2M_N) \langle N, \uparrow | J^+ | N, \downarrow \rangle$, with nucleon light-cone spinors, and in a frame with $q^+ = 0$ and $Q^2 = \mathbf{q}_\perp^2 = q_x^2$.

The model nucleon consists of three relativistically moving, bound constituent quarks, which are surrounded by a cloud of pions. The quark aspects[5]-[9], will be discussed first. The original construction of this three-quark model was based on symmetry principles[5],[6]. The wave function is anti-symmetric, a function of relative momenta, independent of reference frame, and an eigenstate of the spin operator. Schlumpf[7] applied it to compute a variety of baryonic properties. Frank, Jennings & I [8] used this model to predict a very strong decrease of G_E/G_M as a function of Q^2 , which has now been measured. Explaining the meaning of this result was left for a second paper[9] in which imposing Poincaré invariance was shown to lead to an analytic result that the ratio QF_2/F_1 is constant for large Q^2 and to a violation[10] of the helicity conservation rule.

The wave function we use is given by

$$\Psi(p_i) = \Phi(M_0^2)u(p_1)u(p_2)u(p_3)\psi(p_1, p_2, p_3), \quad p_i = \mathbf{p}_i s_i, \tau_i \quad (1)$$

where ψ is a spin-isospin color amplitude factor, the p_i are expressed in terms of relative coordinates, the $u(p_i)$ are ordinary Dirac spinors, Φ is a spatial wave function and the repeated indices p_i are summed over. The specific form of ψ is given in Eq. (12) of Ref. [9] and earlier in Ref. [6] The notation is that $\mathbf{p}_i = (p_i^+, \mathbf{p}_{i\perp})$. The total momentum is $\mathbf{P} = \mathbf{p}_1 + \mathbf{p}_2 + \mathbf{p}_3$. The relative coordinates are $\xi = p_1^+/p_1^+ + p_2^+/p_2^+$, $\eta = (p_1^+ + p_2^+)/P^+$, and $\mathbf{k}_\perp = (1 - \xi)\mathbf{p}_{1\perp} - \xi\mathbf{p}_{2\perp}$, $\mathbf{K}_\perp = (1 - \eta)(\mathbf{p}_{1\perp} + \mathbf{p}_{2\perp}) - \eta\mathbf{p}_{3\perp}$. In computing a form factor, we take quark 3 to be the one struck by the photon. The value of $1 - \eta$ is not changed ($q^+ = 0$), so only one relative momentum, \mathbf{K}_\perp is changed: $\mathbf{K}'_\perp = \mathbf{K}_\perp - \eta\mathbf{q}_\perp$. We take the form of the spatial wave function from Schlumpf[7]: $\Phi(M_0) = \frac{N}{(M_0^2 + \beta^2)^\gamma}$, with M_0^2 is the mass-squared operator for a non-interacting system:

$$M_0^2 = \frac{K_\perp^2}{\eta(1 - \eta)} + \frac{k_\perp^2 + m^2}{\eta\xi(1 - \xi)} + \frac{m^2}{1 - \eta}. \quad (2)$$

Schlumpf's parameters are $\beta = 0.607$ GeV, $\gamma = 3.5$, $m = 0.267$ GeV. The value of γ was chosen that $Q^4 G_M(Q^2)$ is approximately constant for $Q^2 > 4$ GeV² in accord with experimental data. The parameter β helps govern the values of the perp-momenta allowed by the wave function Φ and is closely related to the rms charge radius, and m is mainly determined by the magnetic moment of the proton. We shall use different values when including the pion cloud.

The calculation of form factors is simplified by using completeness to express the wave function in terms of light cone spinors $u_L(p^+, \mathbf{p}, \lambda)$, which are related to Dirac spinors by a unitary Melosh rotation evaluated in terms of Pauli spinors: $|\lambda_i\rangle, |s_i\rangle$, with $\langle\lambda_i|R_M^\dagger(\mathbf{p}_i)|s_i\rangle \equiv \bar{u}_L(\mathbf{p}_i, \lambda_i)u(\mathbf{p}_i, s_i)$. Thus the wave function depends on Melosh rotated Pauli spinors:

$$|\uparrow \mathbf{p}_i\rangle = \left[\frac{m + (1 - \eta)M_0 + i\boldsymbol{\sigma} \cdot (\mathbf{n} \times \mathbf{p}_3)}{\sqrt{(m + (1 - \eta)M_0)^2 + p_{3\perp}^2}} \right] \begin{pmatrix} 1 \\ 0 \end{pmatrix} \quad (3)$$

where the quantity in brackets is $R_M^\dagger(\mathbf{p}_3)$. The spin-isospin wave function can then be thought of as constructed from the non-relativistic quark model, but with the replacement of Pauli spinors by those of Eq. (3). An important effect resides in the term $(\mathbf{n} \times \mathbf{p}_3)$ which originates from the lower components of the Dirac spinors: the orbital angular momentum $L_z \neq 0$ [11]. The term $(\mathbf{n} \times \mathbf{p}_3)$ is also responsible for the flatness of the ratio $F_2(Q^2)/F_1(Q^2)$.

We turn now to neutron properties. The three-quark model for the proton respects charge symmetry, invariance under the interchange of u and d quarks, so it contains a prediction, shown in Fig. 1 (compared with data from Ref. [12]) for neutron form factors. We note that G_{E_n} would vanish in the non-relativistic limit, $R_M \rightarrow 1$, so the deviations from 0 are solely due to relativistic effects. The resulting electric form factor, shown in the curve labeled relativistic quarks, is very small at low values of Q^2 , but at larger values of Q^2 the prediction is larger than that of the Galster parametrization[13].

The slope of G_{E_n} is related to the charge radius as $G_{E_n}(Q^2) \rightarrow -Q^2 R_n^2/6$ with a measured value[14] of $R_n^2 = -0.113 \pm 0.005$ fm². The three-quark model value is -0.025 fm². To understand this small magnitude we express G_E in terms of $F_{1,2}$ for small values of Q^2 . Then $R_n^2 = R_1^2 + R_F^2$, where the Foldy

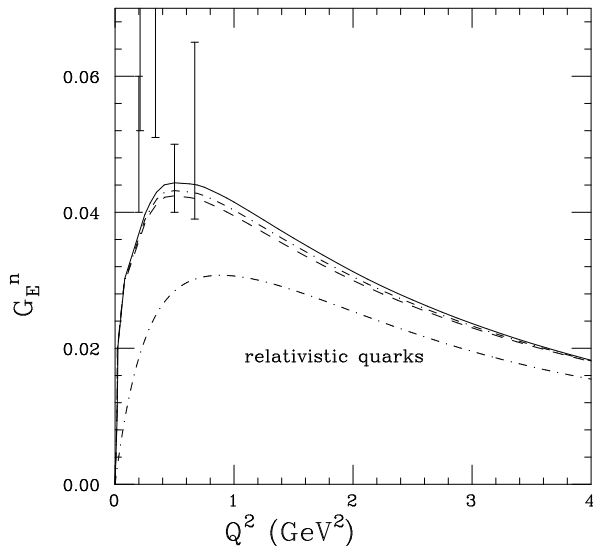


Figure 1: Calculation of G_E^n . The data are from Ref. [12].

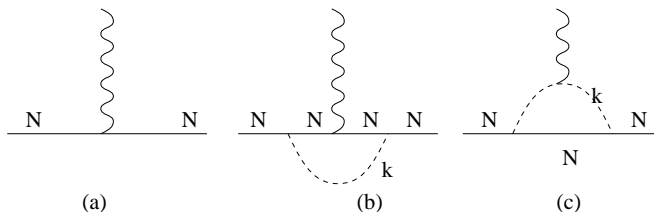


Figure 2: Diagrams

contribution, $R_F^2 = 6\kappa_n/4M^2 = -0.111 \text{ fm}^2$ is, by itself, in good agreement with the experimental data. But this does not guarantee success in explaining the charge radius because one needs to include the Q^2 dependence of F_1 which gives R_1^2 . In the three-quark model $R_1^2 = +0.086 \text{ fm}^2$ which nearly cancels the effects of R_F^2 . Such a cancellation is a natural consequence of including the relativistic effects of the lower components of the quark Dirac spinors[15]. Another effect is needed.

Sometimes a physical nucleon can be a bare nucleon emersed in a pion cloud. An incident photon can interact electromagnetically with a bare nucleon, Fig. 2a, with a nucleon while a pion is present, Fig. 2b, or with a charged pion in flight, Fig. 2c. These effects are especially pronounced for the neutron G_E [16], at small values of Q^2 , because the quark effects are small. The tail of the negatively charged pion distribution extends far out into space, causing R_n^2 to be negative. Such contributions were computed long ago using the cloudy bag model[16], which employed static nucleons.

It is necessary to compute the effects of the pion cloud in a relativistic manner, to confront data taken at large Q^2 . This involves evaluating the Feynman diagrams of Fig. 2 using photon-nucleon form factors from our relativistic model, and using a relativistic π -nucleon form factor. We define the resulting model as the light-front cloudy bag model LFCBM. The light-front treatment is implemented by doing the integral over the virtual pion four-momentum k^\pm, \mathbf{k}_\perp performing the integral over k^- analytically, re-expressing the remaining integrals in terms of relative variables ($\alpha = k^+/P^+$), and shifting the relative \perp variable to \mathbf{L}_\perp to simplify the numerators. Thus the Feynman graphs, Fig. 2, are represented by a single τ -ordered diagram. The use of J^+ and the Yan identity[17] $S_F(p) = \sum_s u(p, s)\bar{u}(p, s)/(p^2 - m^2 + i\epsilon) + \gamma^+/2p^+$ allows one see that the nucleon current operators appearing in Fig.2b act between on-mass-shell spinors.

The results can be stated as

$$F_{i\alpha}(Q^2) = Z \left[F_{i\alpha}^{(0)}(Q^2) + F_{ib\alpha}(Q^2) + F_{ic\alpha}(Q^2) \right], \quad (4)$$

Table 1: Different parameter sets, units in terms of fm

<i>Set(legend)</i>	m	β	Λ	γ	$-R_n^2$	$-\mu_n$	μ_p
1 solid	1.8	3.65	3.1	4.1	0.111	1.73	2.88
2 dot-dash	1.7	3.4	3.1	3.9	0.110	1.79	2.95
3 dash	1.7	2.65	3.1	3.7	0.109	1.79	2.95

where $i = 1, 2$ denotes the Dirac and Pauli form factors, $\alpha = n, p$ determines the identity of the nucleon, and $F_{i\alpha}^{(0)}(Q^2)$ are the form factors computed in the absence of pionic effects. The wave function renormalization constant Z is determined from the condition the charge of the proton be unity: $F_{1p}(Q^2 = 0) = 1$. Calculating the graph Fig. 2b gives

$$F_{1bn}(Q^2) = (2F_{1p}^{(0)}(Q^2) + F_{1n}^{(0)}(Q^2)) \int_N (\alpha^2 M^2 + L_\perp^2 - \alpha^2 Q^2/4) \\ + (2F_{2p}^{(0)}(Q^2) + F_{2n}^{(0)}(Q^2)) \int_N (\alpha^2 Q^2/2), \quad (5)$$

$$F_{2bn}(Q^2) = (F_{1p}^{(0)}(Q^2) + F_{1n}^{(0)}(Q^2)/2) \int_N (2M^2 \alpha^2) + (F_{2p}^{(0)}(Q^2) + F_{2n}^{(0)}(Q^2)/2) \int_N (4\alpha^2 M^2 + 2\mu^2). \quad (6)$$

where the integration measure \int_N is given by

$$\int_N \equiv \frac{g^2}{2(2\pi)^3} \int d^2 L_\perp \frac{d\alpha}{\alpha} R(\mathbf{L}_\perp^{(+)}, \alpha) R(\mathbf{L}_\perp^{(-)}, \alpha), \quad (7)$$

g is the πN coupling constant, $g^2/4\pi = 14$, $\mathbf{L}_\perp^{(\pm)} \equiv \mathbf{L}_\perp \pm \alpha \mathbf{q}_\perp/2$, $\alpha D(k_\perp^2, \alpha) \equiv M^2 \alpha^2 + k_\perp^2 + \mu^2(1 - \alpha)$, and $R(k_\perp^2, \alpha) \equiv \frac{F_{\pi N}(k_\perp^2, \alpha)}{D(k_\perp^2, \alpha)}$. The πN form factor is taken as

$$F_{\pi N}(k_\perp^2, \alpha) = \exp[-(D(k_\perp^2, \alpha)/2(1 - \alpha)\Lambda^2)], \quad (8)$$

as used by Refs. [18] and [19], and satisfies the constraints needed to maintain charge conservation[20]. Including the form factor this way uses the assumption that the form factor is an analytic function of k^- . The results (5,6) show that each term in the nucleon current operator contributes to both F_1 and F_2 . The evaluation of graph 2c yields

$$F_{1cn}(Q^2) = -2F_\pi(Q^2) \int_N \frac{(1 - \alpha)}{\alpha} (\alpha^2 M^2 + L_\perp^2 - (1 - \alpha)Q^2/4) \quad (9)$$

$$F_{2cn}(Q^2) = -2F_\pi(Q^2) \int_N \frac{(1 - \alpha)}{\alpha} (2m^2 \alpha(1 - \alpha)). \quad (10)$$

The proton form factors can be obtained by simply making the replacements $n \rightarrow p$ in Eqs. (5,6) and $-2 \rightarrow +2$ in Eqs. (9,10).

Eqs. (4-10) completely specify the form of the calculation. But the LFCBM requires four parameters $m, \beta, \gamma, \Lambda$. Including pionic effects while continuing to use the original values of m, β, γ , would lead to a satisfactory description of G_{En} [11], but would cause other computed observables to disagree with experiment. Thus a new set of parameters is needed. The following set of requirements is used to restrict the parameters. First, the magnetic moments of the proton and neutron must agree with measured ones within 10%. We also require that the computed values of $G_{Mn}(0.5)$, $G_{En}(1, 1.5)$, $G_{Mn}(4)$, $\mu G_{Ep}/G_{Mp}(5.5)$, $G_{Mp}(5.5)$ and $G_{Mp}(10)$ agree with the measured values well enough so that the average disagreement is about one error bar. There are many parameter sets that satisfy this criterion. We show results for three in Table 1[21] and in the figures.

The first application of the LFCBM is to G_{En} and the results of using the three parameters sets of Table 1 are shown in Fig. 1. It is easy to find many parameters which provide a large pionic effect at

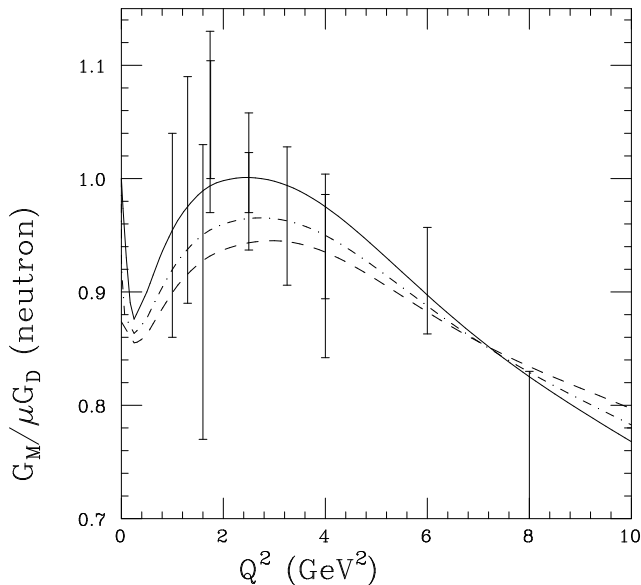


Figure 3: $G_{Mn}/\mu G_D$ for the neutron. Data are from Ref. [22].

small values of Q^2 . The agreement with existing data is good, and more higher quality data at larger values of Q^2 is expected[3]. The next step is to compute G_{Mn} , which is expressed as $G_{Mn}/\mu G_D$, where μ is the computed neutron magnetic moment and $G_D = (1 + Q^2/0.71\text{GeV}^2)^{-2}$. The results are shown in Fig. 3. The agreement between the present theory and existing data [22] is excellent, but this will soon be tested by a new experiment[4].

We turn now to the calculation of proton observables. Fig. 4 shows that the measured ratio of Dirac to Pauli form factors is reasonably well-reproduced. This is very similar to our earlier results[8, 9], showing that the pion cloud effects are not very important for this ratio at relatively large values of Q^2 . These ratios are insensitive to the parameter set, and the results for sets 2 and 3 overlap. Thus, as stressed elsewhere[9, 11] respecting symmetries is more important than including detailed dynamics in obtaining a constant ratio. Finally, the proton magnetic form factor, expressed as $G_M/\mu G_D$, where μ is the computed proton magnetic moment, is shown in Fig. 5. For this case, set 3 seems to provide a “best” description of the present data[23] up to about $Q^2 = 20 \text{ GeV}^2$. For higher values the calculation falls a bit below the data, perhaps indicating the need for the effects of perturbative QCD.

These calculations show that the combination of Poincaré invariance and chiral symmetry, as realized in the present light front cloudy bag model, is sufficient to describe the existing experimental data up to about $Q^2 = 20 \text{ GeV}^2$. This is somewhat surprising as the model keeps only two necessary effects. The effects of mixing of quark-configurations[24], the variation of the quark mass with Q^2 [25], exchange currents[27] and an intermediate Δ [16] could enter, but these seem to have little influence within our model.

Perhaps the strongest feature of the model is that it is testable in upcoming experiments. For the proton, QF_2/F_1 is predicted to be constant for values of Q^2 up to about 20 GeV^2 . The neutron G_{En} , soon to be measured, is predicted as is its magnetic form factor also soon to be measured.

There also are implications for other reactions. Hadron helicity conservation predicts that $Q^2 F_2/F_1$ is constant[26]. This is not respected in present data, so there is no need to expect it to hold for a variety of exclusive reactions occurring at high $Q^2 \leq 5.5 \text{ GeV}^2$. Examples include the large spin effects observed in pp elastic scattering[28] and the reaction $\gamma d \rightarrow np$ [29], but there are many other possibilities.

Acknowledgments

This work is partially supported by the U.S. DOE. I thank R. Madey for encouraging me to compute G_E^n .

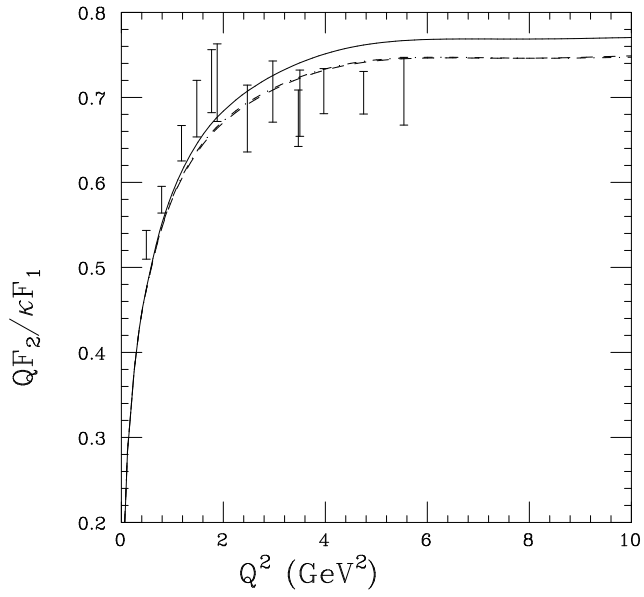


Figure 4: $QF_2/\kappa F_1$ for proton. Data are from Refs. [1, 2].

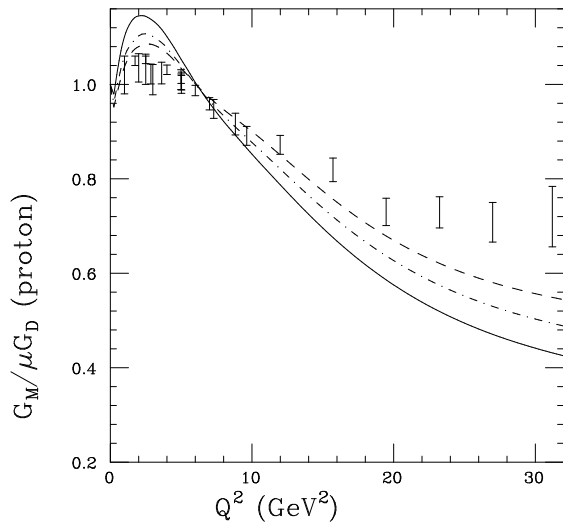


Figure 5: $G_{Mp}/\mu G_D$. Data are from Ref. [23]

References

- [1] M. K. Jones *et al.*, Phys. Rev. Lett. **84**, 1398 (2000)
- [2] O. Gayou *et al.*, Phys. Rev. Lett. **88**, 092301 (2002).
- [3] R. Madey, Spokesperson, Jlab experiment E93-038 D. Day, Spokesperson, Jlab experiment E93-026. B. Reitz, B. Wojtsekhowski, and G. Cates, Spokesmen, Jlab experiment E02-013.
- [4] W. Brooks and M. Vineyard, Jlab experiment E94-017
- [5] V. B. Berestetskii and M. V. Terent'ev. Sov. J. Nucl. Phys. **25**, 347 (1977).
- [6] P. L. Chung and F. Coester. Phys. Rev. D **44**, 229, (1991).
- [7] F. Schlumpf, U. Zurich Ph. D. Thesis, hep-ph/9211255.
- [8] M.R. Frank, B.K. Jennings and G.A. Miller, Phys. Rev. C **54**, 920 (1996).
- [9] G. A. Miller and M. R. Frank, Phys. Rev. C **65**, 065205 (2002)
- [10] T. Gousset, B. Pire and J. P. Ralston, Phys. Rev. D **53**, 1202 (1996)
- [11] G. A. Miller, arXiv:nucl-th/0206027.
- [12] C. Herberg *et al.*, Eur. Phys. J. A **5**, 131 (1999). M. Ostrick *et al.*, Phys. Rev. Lett. **83**, 276 (1999). I. Passchier *et al.*, Phys. Rev. Lett. **82**, 4988 (1999) D. Rohe *et al.*, Phys. Rev. Lett. **83**, 4257 (1999). H. Zhu *et al.* Phys. Rev. Lett. **87**, 081801 (2001)
- [13] S. Galster *et al.*, Nucl. Phys. B **32**, 221 (1971).
- [14] S. Kopecky *et al.*, Phys. Rev. Lett. **74**, 2427 (1995)
- [15] N. Isgur, Phys. Rev. Lett. **83**, 272 (1999)
- [16] S. Th  berge, A. W. Thomas and G. A. Miller, Phys. Rev. **D22** (1980) 2838; (1981) 2106, A. W. Thomas, S. Th  berge, and G. A. Miller, Phys. Rev. **D24** (1981) 216; S. Th  berge, G. A. Miller and A. W. Thomas, Can. J. Phys. **60**, 59 (1982). G. A. Miller, A. W. Thomas and S. Th  berge, Phys. Lett. B **91**, 192 (1980).
- [17] S. J. Chang and T. M. Yan, Phys. Rev. D **7**, 1147 (1973).
- [18] V. R. Zoller, Z. Phys. C **53**, 443 (1992).
- [19] H. Holtmann, A. Szczurek and J. Speth, Nucl. Phys. A **596**, 631 (1996) [arXiv:hep-ph/9601388].
- [20] J. Speth and A. W. Thomas, Adv. Nucl. Phys. **24**, 83 (1997).
- [21] The author will make available the computer program lfcbm.f to any researcher wishing to choose different parameters.
- [22] A. Lung *et al.*, Phys. Rev. Lett. **70**, 718 (1993). S. Rock *et al.*, Phys. Rev. D **46**, 24 (1992). P. E. Bosted, Phys. Rev. C **51**, 409 (1995). R. G. Arnold *et al.*, Phys. Rev. Lett. **61**, 806 (1988).
- [23] W. Bartel *et al.*, Nucl. Phys. B **58**, 429 (1973). A. F. Sill *et al.*, Phys. Rev. D **48**, 29 (1993). L. Andivahis *et al.*, Phys. Rev. D **50**, 5491 (1994). R. C. Walker *et al.*, Phys. Rev. D **49**, 5671 (1994).
- [24] F. Cardarelli and S. Simula, Phys. Rev. C **62**, 065201 (2000)
- [25] J. C. Bloch, C. D. Roberts, S. M. Schmidt, A. Bender and M. R. Frank, Phys. Rev. C **60**, 062201 (1999); C. D. Roberts, and S. M. Schmidt, Prog. Part. Nucl. Phys. **45**, S1 (2000).
- [26] G. P. Lepage and S. J. Brodsky, Phys. Rev. D **22**, 2157 (1980);
- [27] W. R. de Araujo, E. F. Suisso, T. Frederico, M. Beyer and H. J. Weber, Phys. Lett. B **478**, 86 (2000); E. F. Suisso, W. R. de Araujo, T. Frederico, M. Beyer and H. J. Weber, Nucl. Phys. A **694**, 351 (2001); K. Bodoor, H. J. Weber, T. Frederico and M. Beyer, Mod. Phys. Lett. A **15**, 2191 (2000)
- [28] E. A. Crosbie *et al.*, Phys. Rev. D **23**, 600 (1981).
- [29] K. Wijesooriya *et al.* [Jefferson Lab Hall A Collaboration], Phys. Rev. Lett. **86**, 2975 (2001).